Dyes and Pigments 190 (2021) 109335

Contents lists available at ScienceDirect

Dyes and Pigments

journal homepage: http://www.elsevier.com/locate/dyepig

Development of a coumarin-based fluorescent probe for hydrogen peroxide based on the Payne/Dakin tandem reaction

Fangfang Wu [a], Hanjie Yu [b], Qin Wang [c], Jianjian Zhang [a], Zheng Li [b], Xiao-Feng Yang [a,*]

[a] Key Laboratory of Synthetic and Natural Functional Molecule Chemistry of Ministry of Education, College of Chemistry & Materials Science, Northwest University, Xi'an, 710127, PR China
[b] Laboratory for Functional Glycomics, College of Life Sciences, Northwest University, Xi'an, 710069, PR China
[c] Shaanxi Key Laboratory of Catalysis, School of Chemistry and Environment Science, Shaanxi University of Technology, Hanzhong, Shaanxi, 723000, PR China

ARTICLE INFO

Keywords:
Hydrogen peroxide
Fluorescent probe
Payne reaction
Dakin reaction
Coumarin
Cell imaging

ABSTRACT

Hydrogen peroxide (H_2O_2) is associated with many physiological and pathological processes in biological systems. Here, we report 7-diethylamino-3-formyl-coumarin (**Cou-CHO**) as a turn-on fluorescent probe for H_2O_2. The proposed probe employs a tandem Payne/Dakin reaction to convert the electron-withdrawing aldehyde to the electron-donating hydroxyl group, thus hindering the formation of twisted intramolecular charge transfer (TICT) state of 7-diethylaminocoumarin, and thereby resulting in a fluorescence turn-on response. **Cou-CHO** features high specificity, excellent sensitivity and fast response toward H_2O_2. In particular, **Cou-CHO** enables the direct visualization of basal and endogenously produced H_2O_2 in living cells. The results demonstrate that the tandem Payne/Dakin reaction can provide a new choice to develop H_2O_2-selective probes.

1. Introduction

Hydrogen peroxide (H_2O_2), as an important reactive oxygen species (ROS), is mainly generated in mitochondria by the activation of nicotinamide adenine dinucleotide phosphate (NADPH) oxidase complex [1], and can diffuse across cellular membranes to regulate a large variety of physiological processes from the immune response to cell signaling [2]. However, aberrant production of H_2O_2 is involved in many diseases, such as cardiovascular disorders, diabetes, Parkinson's disease, Alzheimer's disease, Huntington's disease, metabolic diseases and cancers [3,4]. Thus, it is of great importance to develop chemical tools to detect H_2O_2 in living systems.

Fluorescent probes offer powerful chemical tools for monitoring biological species in living biosystems, owing to their simplicity, high sensitivity, high spatial resolution, and noninvasiveness. So far, several fluorescent probes have been developed for H_2O_2 detection and imaging [5–7], which employs boronic esters/acid [8,9], benzyl [10], aryl sulfonyl esters [11,12] and α-ketoamide [13] as the recognition unit. However, as H_2O_2 exhibits relatively mild reactivity among ROS, most H_2O_2 probes give a sluggish response and have drawbacks in terms of selectivity. For instance, some boronate-based probes respond to H_2O_2 more slowly when compare to other more reactive species, such as peroxynitrite ($ONOO^-$) and hypochlorous acid (HClO) [14,15]. In fact, the utilization of boronate (or boronic acid) as a recognition unit for $ONOO^-$ [16,17] or benzoyl peroxide [18] have been reported. Similarly, α-ketoamide-based H_2O_2 probes were also reported for $ONOO^-$ detection [19,20], because $ONOO^-$ is reported to possess much stronger nucleophilicity than H_2O_2 under physiological conditions [15]. Therefore, the development of H_2O_2 fluorescent probes with new reaction mechanisms is highly desirable.

Recently, Yang et al. reported an innovative probe for H_2O_2 based on a tandem Payne/Dakin reaction coupled with the traditional rhodamine decaging method [21]. The overall strategy employs a specific H_2O_2-mediated transformation of benzaldehydes into the corresponding phenols, which subsequently undergoes a spontaneous 1,6-elimination and carbamate cleavage to release the fluorophore, resulting in a dramatic fluorescence enhancement. Inspired by the above strategy, we envisioned that the above functionality transformation from the electron-withdrawing aldehyde to the electron-donating hydroxyl group might serve as a promising chemical handle for constructing H_2O_2 probes directly, because the pronounced change in electronic properties of the function group may influence the photophysical states of a fluorophore, which should in turn lead to observable changes in its optical properties.

In this work, we report 7-diethylamino-3-formyl-coumarin (**Cou-CHO**) as a new turn-on fluorescent probe for H_2O_2. In aqueous polar

* Corresponding author.
E-mail address: xfyang@nwu.edu.cn (X.-F. Yang).

https://doi.org/10.1016/j.dyepig.2021.109335
Received 18 January 2021; Received in revised form 15 March 2021; Accepted 16 March 2021
Available online 24 March 2021

solvents, **Cou-CHO** is weakly emissive due to the formation of the twisted intramolecular charge transfer (TICT) state upon photoexcitation. Upon mixing with H_2O_2 in the presence of trichloroacetonitrile (CCl_3CN), trichloroperoxyacetamidic acid (TCPAA) is formed from the reaction of CCl_3CN with H_2O_2 (Payne reaction), which then affords a Dakin oxidation via nucleophilic attack of the aldehyde on the 3-position of **Cou-CHO** by its anion form, and subsequent hydrolysis of the intermediate gives the corresponding **Cou-OH** as the final product. This tandem reaction converts the electron-withdrawing aldehyde moiety of **Cou-CHO** to the electron-donating hydroxyl group, thus hindering formation of the TICT state and thereby resulting in a significant fluorescence enhancement (Scheme 1). The fluorescent intensity at 502 nm increases linearly with H_2O_2 concentration in the range 0.5–10 μM. The proposed probe exhibits excellent selectivity toward H_2O_2 over other ROS, reactive nitrogen species (RNS) and related biological species. The practical utility of **Cou-CHO** in biological contexts has been demonstrated by imaging basal and endogenous H_2O_2 in living cells.

2. Experimental section

2.1. General procedure for spectral measurements

The stock solution of **Cou-CHO** (1 mM) was prepared in acetone. H_2O_2 solution was dissolved in deionized water directly, and its concentration was identified from the absorption at 240 nm (ε = 43.6 $M^{-1}cm^{-1}$). Other ROS/RNS were also prepared according to the previous reported method [22]. A typical test solution was prepared by adding 25 μL of **Cou-CHO** (1 mM), 1.5 mL of ethanol, 0.5 mL of 0.2 M phosphate buffer (0.2 M, pH 7.4), 50 μL of CCl_3CN (100 μM), and a required volume of test species sample solution. The above solution was diluted to 5.0 mL with water and maintained at 37 °C for 20 min. And then the absorption or fluorescence spectra were recorded.

2.2. Cell imaging experiments

HepG2 cells were plated on plastic Petri dishes and allowed to attach for a day before the imaging experiment. The cells were then incubated with **Cou-CHO** (5 μM) in FBS-free RPMI for 30 min then washed with PBS (pH 7.4) three times. For imaging of exogenous H_2O_2, the cells were then treated with different concentration of H_2O_2 (5, 10, 20 μM) in the presence of CCl_3CN (100 μM) in PBS buffer for 30 min. After washing the cells with PBS buffer three times, cell imaging was then carried out under a confocal fluorescence microscope with an objective lens (× 40). The fluorescence emission was collected at 470–520 nm upon excitation at 405 nm. For imaging endogenous H_2O_2 generation in HepG2 cells, the cells were pretreated with phorbol-12-myristate-13-acetate (PMA, 0.5 μg mL^{-1}) or rotenone (RO, 0.5 μM) for 30 min, and then incubated with the probe in the presence of CCl_3CN (100 μM) for 30 min. For the scavenging assay, the cells were co-incubated with the stimulator (PMA or RO) and N-acetylcysteine (NAC, 1 mM) for 30 min, and then treated with the probe and CCl_3CN as described above. Cell images were captured after the cells were washed with PBS three times.

3. Result and discussion

3.1. Development of fluorescent probes for H_2O_2

Compared with other ROS, H_2O_2 is a relatively stable species and exhibits mild reactivity. Therefore, fluorescent probes for H_2O_2 are liable to be interfered upon by highly reactive species, such as $ONOO^-$. Recently, Yang et al. reported a new approach to H_2O_2 recognition based on a tandem Payne/Dakin reaction [21,23]. H_2O_2 can be activated by the in situ formation of a sufficiently reactive trichloroperoxyacetamidic acid (TCPAA) from its addition to trichloroacetonitrile (CCl_3CN) in neutral aqueous media [24]. Subsequently, TCPAA can afford a Dakin reaction to give the corresponding phenol, which initiates the following 1,6-elimination to release the fluorescent conjugated xanthene ring and emits strong fluorescence. The above synergistic Payne/Dakin reactions afford the transformation of aldehydes (-CHO) into the corresponding hydroxyl groups (-OH), which serves as the basis for sensitive and specific H_2O_2 detection. However, in the above design strategy, the functionality transformation and the decaging of xanthene dyes have to be integrated to achieve the sensing purpose, which makes the probe design complicated and lengthy synthesis has to be carried out. This encourages us to improve the above strategy to realize much advanced H_2O_2 probes.

In fact, the functional group transformation represents a new approach for developing selective probes in biological systems. The aldehyde is a typical electron-deficient group, while the hydroxyl group is an electron-donating one. Thus, we envisioned that the above change in electronic properties of the function group via tandem Payne/Dakin reactions may influence the photophysical properties of a fluorophore, thus producing a discernible change in its emission properties. This might be an effective signaling mechanism and could be employed to devise H_2O_2 fluorescent probes.

It is well-known that 7-dialkylaminiocoumarins are solvatochromic dyes, which undergoes a nonradiative rotational (twisting) decay mechanism that leads to full charge separation in the excited state [25]. In general, due to the formation of this twisted intramolecular charge transfer (TICT) state, 7-dialkylaminiocoumarins are weakly emissive in highly polar solvents [26]. It was further reported that the fluorescence

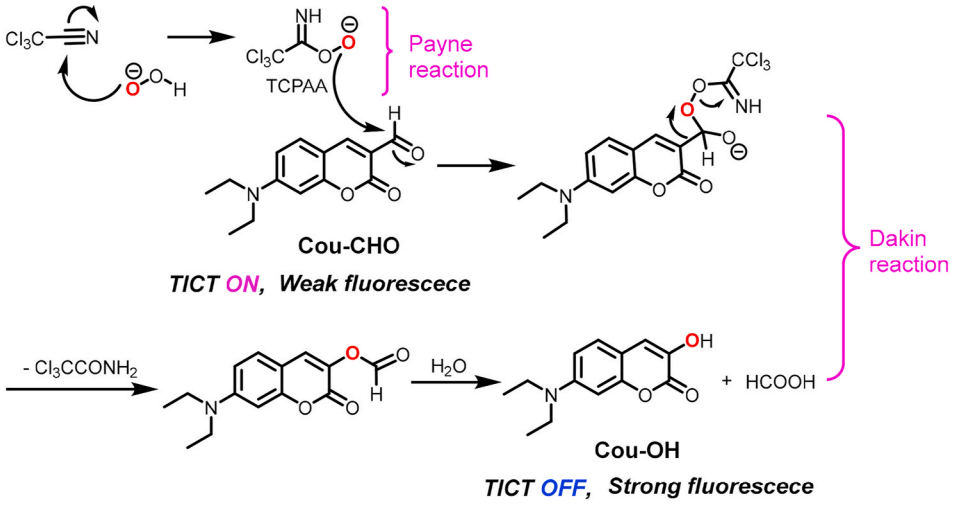

Scheme 1. Proposed reaction mechanism for sensing of H_2O_2 when using **Cou-CHO**.

properties of these fluorophores can be varied by the strength of the electron-withdrawing substituents at its 3-position [27,28]. A stronger electron-withdrawing substituent would result in a greater charge transfer from the electron-donating moiety of the aminocoumarin molecule, thus affording weaker fluorescence emission in aqueous media. We reasoned that the functionality transformation from the electron-deficient aldehydes to the electron-donating hydroxyl groups induced by the tandem Payne/Dakin reaction may reduce the electron-withdrawing strength of the substituent, and the twisting relaxational motion may not take place, which in turn leads to a large wavelength shift in the emission spectrum of the probe as well as a turn-on fluorescence response (Scheme 1). The detailed sensing mechanism is depicted in Scheme 1. Based on the above considerations, **Cou-CHO** might be an ideal candidate for H_2O_2 detection via a tandem Payne/Dakin reaction.

To assess the validity of this assumption, compounds **Cou-CHO** and **Cou-OH** were prepared (Scheme 2, the detailed synthetic procedures are shown in Supplementary Data) and their photophysical data were compared at the same conditions. Fig. 1a shows the UV–vis absorption spectra of **Cou-CHO** and **Cou-CHO** in phosphate buffer (pH 7.4, 30% ethanol). **Cou-CHO** exhibits intense absorption band at 448 nm, which is apparently attributed to ICT. However, the absorption spectrum of **Cou-OH** has a marked hypochromatic shift (~70 nm) when compared to **Cou-CHO**. This blueshift is apparently attributed to interrupt of the ICT process within the molecule. Furthermore, the fluorescence spectra of compounds **Cou-CHO** and **Cou-OH** were recorded. It was observed that they display similar emission maximum wavelengths (*ca.* 500 nm); however, the emission intensity of **Cou-OH** is much higher than that of **Cou-CHO** (Fig. 1b). The above results are compiled in Table 1. To our delight, it was further observed that **Cou-CHO** exhibited almost no fluorescence emission upon excitation at the absorption band of **Cou-OH**, which is favorable for the determination of low concentration of H_2O_2. The above results implied that **Cou-CHO** might be employed for H_2O_2 detection with a turn-on fluorescence response, provided that its aldehyde group could be transformed to the hydroxyl group.

3.2. Sensing response to H_2O_2

To examine its usefulness for H_2O_2 detection, **Cou-CHO** was incubated with H_2O_2 in phosphate buffer (20 mM, pH 7.4, with 30% ethanol, 100 μM CCl_3CN) at 37 °C. As shown in Fig. 2a, the maxima absorption of **Cou-CHO** is centered at 448 nm. However, with the addition of increasing concentrations of H_2O_2 (0–15 μM), its absorption maximum at 448 nm progressively decreased with the concomitant formation of a new absorption band at around 378 nm. This spectral variation is apparently due to the disruption of the electron donor-acceptor system within the probe. Meanwhile, changes in the fluorescence spectra of **Cou-CHO** upon treating with increasing concentrations of H_2O_2 were investigated. As indicated in Fig. 2b, the solution of **Cou-CHO** is almost non-fluorescent when excited at 391 nm. Upon addition of H_2O_2, the emission intensity of **Cou-CHO** solution at 502 nm enhanced gradually with increasing concentration of H_2O_2 until a plateau is reached at 10 μM. There is a ca. 34-fold increase in the fluorescence intensity in the presence of 2 equiv. of H_2O_2. The fluorescence intensity at 502 nm increased linearly with the concentration of H_2O_2 in the range 0.5–10 μM, and the detection limit was determined to be 31 nM (3δ). Clearly, these results indicate that **Cou-CHO** can be used to detect H_2O_2 with high sensitivity.

Further, the kinetic behavior of the reaction system was investigated. With the addition of H_2O_2, the intensity of the reaction solution increased significantly. A kinetic assay revealed that the fluorescence at 502 nm reached a maximum after approximately 20 min (Fig. 3). In contrast, the **Cou-CHO** solution alone exhibited no observable fluorescence changes under identical conditions. In addition, time-dependent absorption spectral changes of **Cou-CHO** in the presence of H_2O_2 were recorded. As shown in Fig. S1, the increased of the absorption band at 378 nm and a gradual decline at 448 nm were observed simultaneously as the reaction time prolonged, and they were saturated after ca. 20 min,

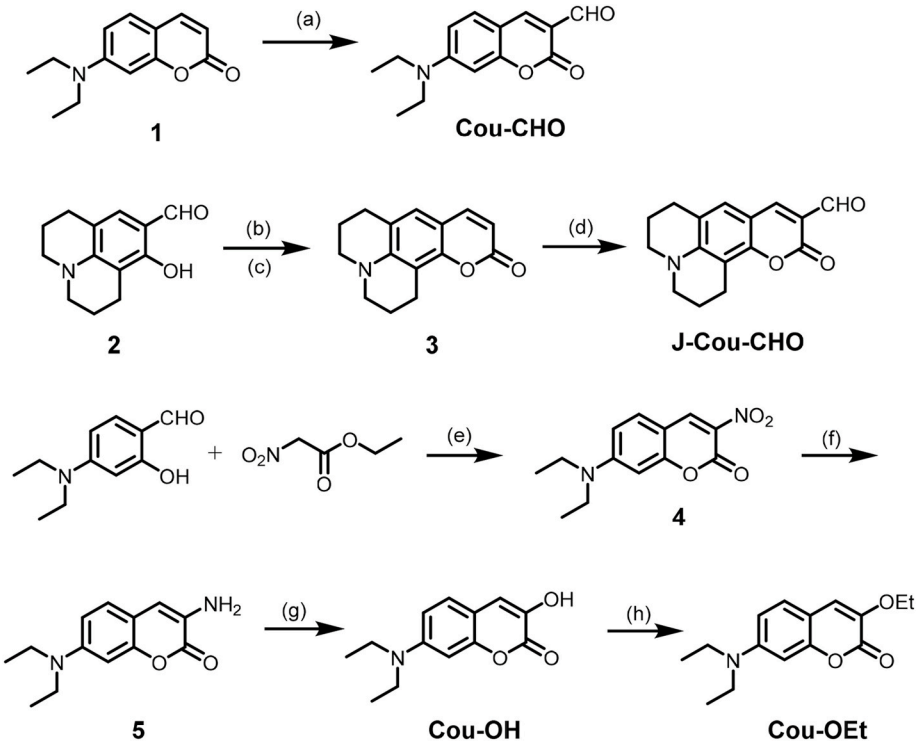

Scheme 2. Synthesis of **Cou-CHO** and control compounds **J-Cou-CHO** and **Cou-OEt**. Conditions: (a) $POCl_3$, DMF; (b) $CH_2(COOEt)_2$, piperidine, reflux 6 h; (c) concentrated HCl, CH_3COOH, reflux 6 h; (d) $POCl_3$, DMF; (e) *n*-butanol, CH_3COOH, piperidine, reflux, 12 h; (f) $SnCl_2$, HCl, room temperature, 2 h; (g) HCl, reflux, 4 h; (h) DMF, EtI, K_2CO_3, 60 °C, 7 h.

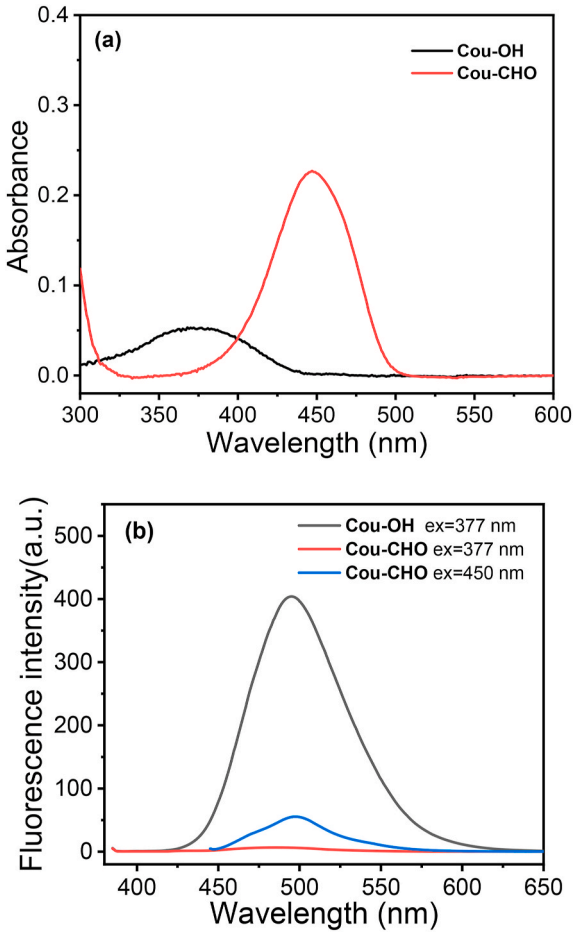

Fig. 1. Absorption (a) and fluorescence spectra (b) of **Cou-CHO** and **Cou-OH** (both 5 μM) in 20 mM phosphate buffer (pH 7.4, 30% ethanol).

Table 1
Photophysical characterization of **Cou-CHO**, **Cou-OH**, **J-Cou-CHO** and **Cou-OEt** in 20 mM phosphate buffer (pH 7.4, 30% ethanol).

Compounds	λ_{abs}/nm[a]	ε_{max}/ × 10^4 $M^{-1}cm^{-1}$	λ_{em}/nm[b]	Φ_F[c]
Cou-CHO	448	4.55	499	0.017
Cou-OH	378	1.05	502	0.26
J-Cou-CHO	464	4.70	513	0.58
Cou-OEt	380	1.01	489	0.24

[a] The maximal absorption of the dye.
[b] The maximal emission of the dye.
[c] Φ_F is the relative fluorescence quantum yield, which was measured by using quinine sulfate ($\Phi_F = 0.55$ in 0.05 M H_2SO_4) as a standard [29].

which was consistent with the results of the fluorescence measurement.

3.3. Effect of pH

The effect of pH on the fluorescence response of **Cou-CHO** to H_2O_2 was investigated. According to the reaction mechanism, the tandem Payne/Dakin reaction should give **Cou-OH** as the final product. Since **Cou-OH** contains a pH-sensitive hydroxyl group at its 3-position, we initially investigate the effect of pH on its fluorescence emission behavior in the pH range of 5.0–9.18. As shown in Fig. S2, the fluorescence signal of **Cou-OH** was strong and stable in the pH range of 5.0–7.0, and decreased markedly when the solution pH is above 7.0. Based on the above data, its pK_a value was determined to be 7.65. The above results indicate that an acidic environment favors the fluorescence measurement of **Cou-OH**, which is unusual in the hydroxyl group-containing

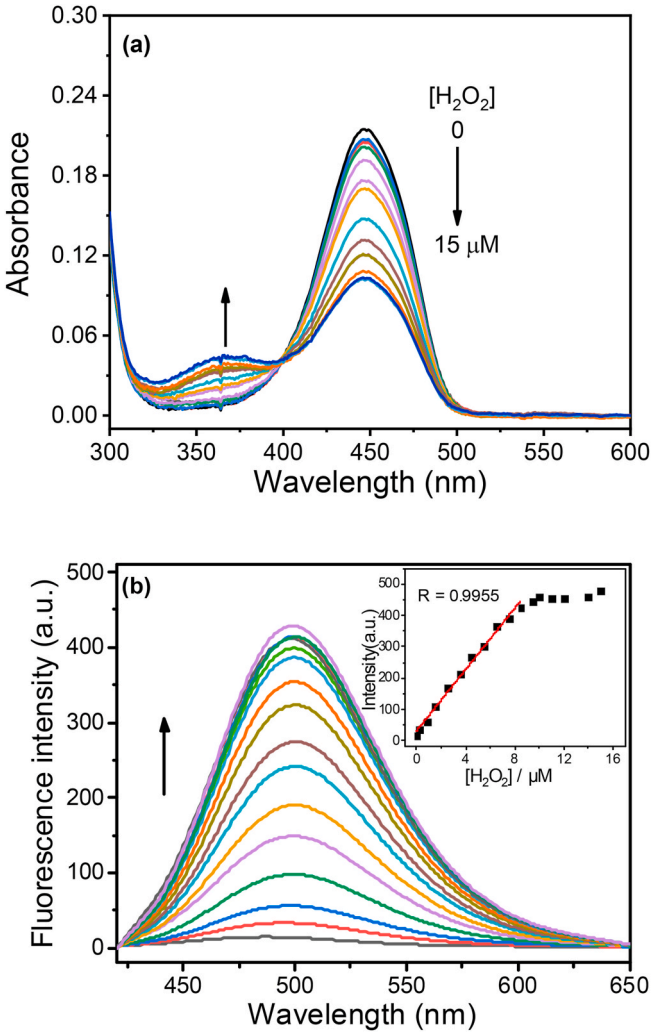

Fig. 2. Absorption (a) and fluorescence spectra (b, $\lambda_{ex} = 391$ nm) of **Cou-CHO** (5 μM) upon treating with increasing concentrations of H_2O_2 (0–15 μM) in 20 mM phosphate buffer (pH 7.4, 30% ethanol, 100 μM CCl_3CN). The reaction was carried out at 37 °C. The spectra were recorded after incubation of **Cou-CHO** with H_2O_2 for 20 min. Inset in (b): fluorescence intensity at 502 nm as a function of H_2O_2 concentration.

fluorescent scaffolds. On the other hand, according to the reaction mechanism, the initial step of Dakin oxidation involves the nucleophilic attack of the aldehyde group by TCPAA in its anion form [30]. Thus, it seems that an alkaline solution favors the Dakin oxidation. Therefore, the effect of pH on the fluorescence signals of the present system was investigated by carrying out the reaction at different pH phosphate buffer solutions (pH: 5.0–9.18). As indicated in Fig. S3, the fluorescence signal increased with pH in the range of 5.6–7.2, thereafter decreased significantly. This is apparently due to the compromise of the above two factors. A relatively strong fluorescence emission was observed in the pH range of 6.5–7.8, which fulfills the requirement for monitoring of H_2O_2 at physiological pH conditions.

3.4. Selectivity studies

The selectivity of **Cou-CHO** toward H_2O_2 was tested by treatment with other potential interfering species in biological system. As shown in Fig. 4 and S4, only H_2O_2 triggers a prominent fluorescence increment, while other ROS and RNS (·OH, $^1O_2$, $O_2^{\cdot-}$, NO, $ONOO^-$, TBHP, TBO· and HClO), metal ions (Ca^{2+}, Cu^{2+}, Fe^{2+}, Fe^{3+}, K^+, Mg^{2+}, Zn^{2+}), and other biological species (SO_3^{2-}, GSH, Cys, Hcy, and His) afford no or minor

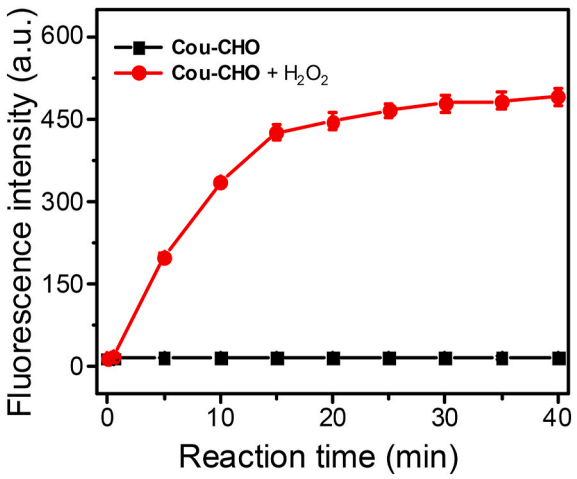

Fig. 3. Time-dependent fluorescence intensity changes of **Cou-CHO** (5 μM) in the presence of H_2O_2 (2 equiv.). The reaction was carried out in 20 mM phosphate buffer (pH 7.4, 30% ethanol, 100 μM CCl_3CN) at 37 °C. $\lambda_{ex}/\lambda_{em}$ = 391/502 nm. Data are represented as mean ± SD (n = 3).

changes under identical conditions. Notably, it was observed that HClO at 100 μM triggered a small fluorescence increment at 481 nm. The above phenomenon might be ascribed to the oxidation of aldehyde to carboxylic group by HClO. However, this reaction has negligible impact towards the selective H_2O_2 detection due to its different emission peak at 481 nm (cf.502 nm using H_2O_2). Although it was reported that bisulfite can react with **Cou-CHO** to afford fluorescence enhancement, the addition reaction has to be carried out in acidic medium (pH 5.0) [31]. Thus, the present sensing system can avoid the interference from bisulfite by carrying out the measurement at physiological pH conditions. In addition, **Cou-CHO** was also reported for Cys/Hcy detection [32]. Nevertheless, it gives turn-off fluorescence response and thus would not interfere with the H_2O_2 detection. Overall, these experiments demonstrate that the present probe has high selectivity for H_2O_2 determination against ROS and RNS, metal ions, and other biological species.

3.5. Mechanistic investigations

The sensing mechanism of the present system was investigated. Initially, some control experiments were carried out to investigate the reaction mechanism. It was observed that treatment of **Cou-CHO** with CCl_3CN or H_2O_2 alone gives no observable changes in fluorescence emission; however, the mixture of CCl_3CN and H_2O_2 exhibits pronounced fluorescence enhancement at 502 nm (Fig. S5). The above results indicate the involvement of TCPAA in the sensing process. Next, according the reaction mechanism, the treatment of **Cou-CHO** with H_2O_2 in the presence of CCl_3CN should give **Cou-OH**. To confirm this, the reaction mixture of **Cou-CHO** and H_2O_2 was subjected to high resolution mass spectrometry. As shown in Fig. S6, a prominent peak at m/z 234.1100 corresponding to **Cou-OH** (calcd. 234.1124 for $C_{13}H_{16}NO_3$) is clearly observed in the HRMS data, indicating the generation of **Cou-OH** in the reaction mixture. Additional proof of the above mechanism is provided by comparing the absorption and emission spectra of the reaction mixture and authentic **Cou-OH**. As shown in Fig. S7, the treatment of **Cou-CHO** with H_2O_2 in the presence of CCl_3CN gives a new absorption band centered at 378 nm, which agrees well the absorption peaks of **Cou-OH**. Further, the emission spectrum of the above reaction solution is identical with that of **Cou-OH**. These results testified to the proposed reaction mechanism shown in Scheme 1.

Now, the key questions related to this reaction is that why the transformation of aldehyde group to hydroxyl group affords a significant turn-on fluorescence response. It was previously reported that the

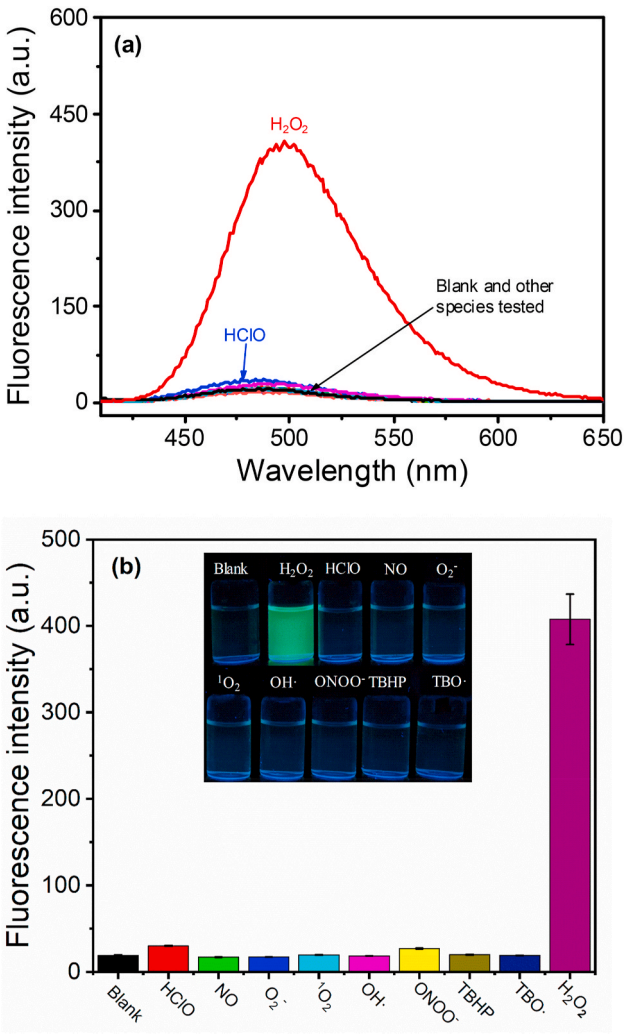

Fig. 4. Fluorescence spectra (a, λ_{ex} = 391 nm) and emission intensity (b) of **Cou-CHO** (5 μM) in the presence of various ROS/RNS (10 μM H_2O_2, 100 μM for other species) in 20 mM phosphate buffer (pH 7.4, 30% ethanol, 100 μM CCl_3CN). Inset in (b): photographs of the solution of **Cou-CHO** after treating with different reactive species under UV light at 365 nm. Data are represented as mean ± SD (n = 3).

hydroxyl group formed in the sensing process could hydrogen bond to the carbonyl in proximity, thus effectively modulating its fluorescence [33–35]. To ascertain this possibility, we prepared **Cou-OEt** (Scheme 2, synthesis and characterization details in Supplementary data), where the hydroxyl group at the 3-position of **Cou-OH** was substituted by an ethoxyl group, and thus precluded the formation of intramolecular hydrogen bond. The fluorescence spectra of **Cou-OEt** and **Cou-OH** were compared in 30% ethanol aqueous solution (pH 7.4). As indicated in Fig. S8, the emission peak of **Cou-OEt** is blue-shifted about 7 nm when compared to **Cou-OH.** However, their fluorescence intensity shows no significant difference. These results indicate the present sensing system is irrelevant to intramolecular hydrogen bond.

On the other hand, previous studies indicate the weak fluorescence of 7-dialkylaminocoumarin is due to the formation of TICT state [26, 36]. To ascertain whether TICT is involved in the present sensing process, we replaced the N,N-diethylamino group at the 7-position of **Cou-CHO** with a bridged julolidinyl moiety (to form **J-Cou-CHO** as a control compound, its synthesis and characterization details are shown in Supplementary data), which would block the rotation of the diethylamino group with respect to the plane of the coumarin skeleton. Thus, the involvement of the TICT state should be excluded [37,38]. The

treatment of **J-Cou-CHO** with H_2O_2 was examined with the same conditions described for **Cou-CHO**. As shown in Fig. S9, **J-Cou-CHO** gives similar absorption variations as that of **Cou-CHO**; however, no fluorescence increase was observed because **J-Cou-CHO** itself has prevented the TICT state formation by incorporation of the nitrogen into a system of fused rings. The above results indicate that the fluorescence enhancement of **Cou-CHO** upon treatment with H_2O_2 is TICT-involved.

In addition to steric hindrance effect, TICT formation in a dye is also governed by its intrinsically electronic effect. The aldehyde group is an electron-withdrawing group, while the hydroxyl group is a typical electron-donating one, thus we reasoned that the transformation of aldehyde to hydroxyl group would increase the energy barrier to enter the TICT state, thus suppressing TICT formation. Generally, the molecules in the TICT excited state have a large dipole moment, and consequently the TICT excited state is stabilized in a polar environment. With the decrease of solution polarity, the energy barrier for torsional motion leading to the TICT state increases; as a result, the TICT process is prohibited, thus leading to an increased fluorescence emission [39,40]. Therefore, the fluorescence properties of **Cou-CHO** and **Cou-OH** were investigated in solvents of different polarities. As shown in Fig. S10, an increase of the 1,4-dioxane percentage in water from 0 to 99%, corresponding to a decrease in solvent polarity, resulted in a hypochromatic shift and fluorescence enhancement for **Cou-CHO** and **Cou-OH**. However, the fluorescence peak intensity of **Cou-CHO** increased 117-fold; whereas for **Cou-OH**, only a 4.2-fold enhancement was observed (Fig. S11), indicating that the former is more sensitive to polarity changes than the latter. These data, therefore, indicate that the turn-on fluorescence response of the present sensing system is apparently due to the inhibition of TICT process within **Cou-CHO** via the functional groups transformation.

3.6. *Fluorescence imaging of H_2O_2 in living cells*

Having confirmed the efficiency of H_2O_2-triggered fluorescence turn-on response, we next moved on to investigate the ability of **Cou-CHO** to visualize H_2O_2 in living cells. Initially, cell cytotoxicity of **Cou-CHO** was evaluated in HepG2 cells by Cell Counting Kit-8 (CCK-8) assays (Fig. S12), and the results suggests the low cytotoxicity of **Cou-CHO** in the concentration range of 0–20 μM (cell viability > 89% for 24 h incubation time). Next, to determine if **Cou-CHO** could react with H_2O_2 in living cells, we stained HepG2 cells with **Cou-CHO** for 30 min, and then exchanged cell media for new media containing varying concentrations of H_2O_2 (5–20 μM). It was observed that cells treated with exogenous H_2O_2 showed a dose-dependent fluorescence turn-on response after 30 min (Fig. 5a and b). There results indicate that **Cou-CHO** reacts with H_2O_2 in living cells to generate a turn-on fluorescence response.

To further confirm its practical usefulness, we assessed the potential ability of **Cou-CHO** for fluorescence imaging of endogenous H_2O_2 in living cells. It was observed that the probe-loaded HepG2 cells displayed observable fluorescence signal (Fig. 6a, first column). In contrast, the cells pretreated with H_2O_2 scavenger NAC showed apparently decreased fluorescence signals (Fig. 6a, second column). The outcome confirms that **Cou-CHO** is capable of imaging intracellular basal H_2O_2. Next, **Cou-CHO** was utilized to image the fluctuation of H_2O_2 in living HepG2 cells. It was reported that PMA can trigger the up-regulation of intracellular H_2O_2 through a cellular inflammation response [41]. Thus, PMA was employed to stimulate the cells and then incubated with the probe. As shown in the third column of Fig. 6a, PMA-stimulated cells showed high levels of fluorescence intensity in comparison with the PMA free cells. The fluorescence increment in the cells was efficiently suppressed by pretreatment with NAC (Fig. 6a, fourth column and Fig. 6b). Furthermore, we stimulated the cells with RO, a high-affinity inhibitor of complex I of the mitochondria electron-transfer chain known to induce the generation of ROS, including H_2O_2 [42]. Similarly, the RO-stimulated cells displayed strong fluorescence and the fluorescence increment could be largely inhibited by NAC (Fig. 6a, fifth and sixth column, Fig. 6b). Taken together, these results support the idea that **Cou-CHO** can monitor endogenous H_2O_2 generation in living cells.

4. Conclusion

To summarize, we have developed a turn-on fluorescent probe for

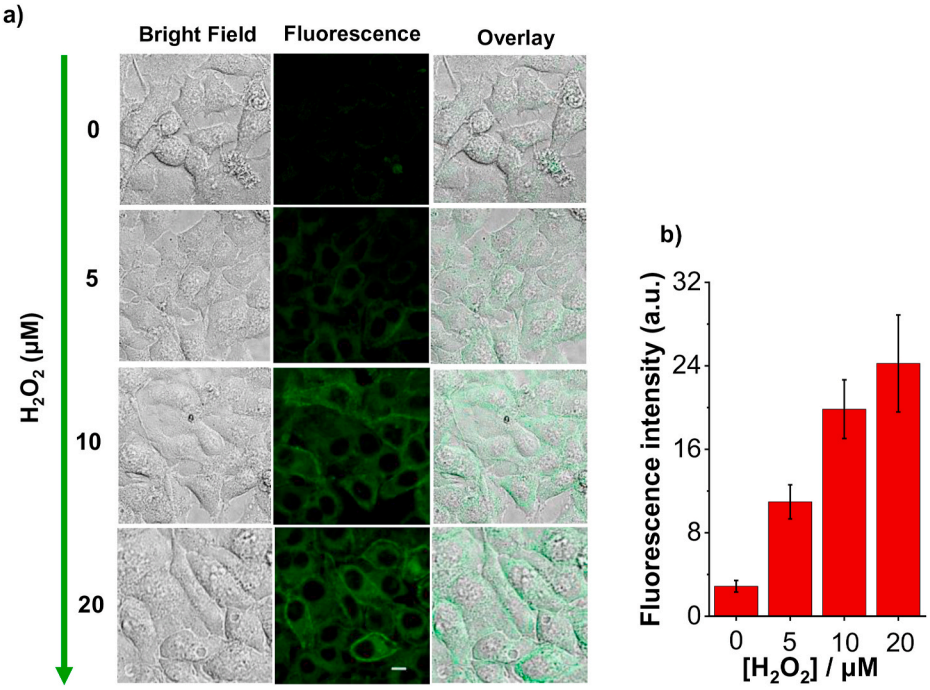

Fig. 5. (a) Fluorescence images of HepG2 cells treated with **Cou-CHO** (5 μM, 30 min) and exposed to a range of H_2O_2 concentrations (0–20 μM) in the presence of CCl_3CN (100 μM) for 30 min λ_{ex} = 405 nm, λ_{em} = 470–520 nm. Scale bar: 20 μm. (b) Relative fluorescence intensity shown in (a) was quantified. The results are shown as mean ± SD (n = 3).

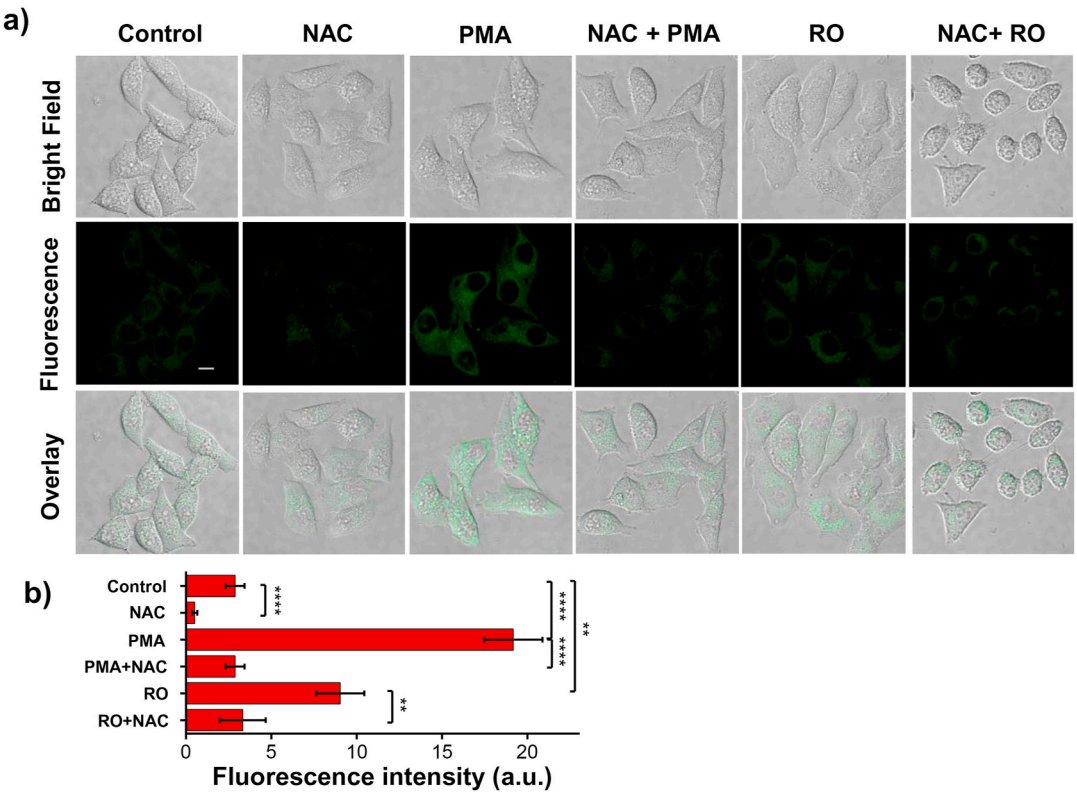

Fig. 6. (a) Fluorescence imaging of endogenous H_2O_2 in HepG2 cells. Cells were pretreated with PBS only (as a control), NAC (1 mM), PMA (0.5 μg/mL), NAC (1 mM) + PMA (0.5 μg/mL), RO (0.5 μM, 0.5 h), NAC (1 mM) + RO (0.5 μM) for 30 min, and further co-incubated with **Cou-CHO** (5 μM, 30 min) and CCl_3CN (100 μM) for 30 min λ_{ex} = 405 nm, λ_{em} = 470–520 nm. Scale bar: 20 μm. (b) Relative fluorescence intensity shown in (a) was quantified. The results are shown as mean ± SD (n = 3). Statistical significance was determined as **p < 0.001, ****p < 0.0001 by student's test.

detecting H_2O_2 in aqueous solutions and living cells. The proposed probe employs a tandem Payne/Dakin reaction to selectively convert the aldehyde to the corresponding hydroxyl group, thus hindering the formation of TICT state of 7-diethylaminocoumarin, and thereby resulting in selective fluorescence turn-on responses to biologically relevant concentrations of H_2O_2 over potentially interfering species. Importantly, the present probe is capable of imaging endogenous H_2O_2 in living cells. We expect that the design strategy described herein can be extended to construct future H_2O_2 fluorescent probes with improved properties.

Credit author statement

Fangfang Wu: Conceptualization, Methodology; Investigation; Writing - Original Draft; **Hanjie Yu**: Investigation, Data curation; **Qin Wang**: Conceptualization, Investigation; **Jianjian Zhang**: Conceptualization, Methodology; **Zheng Li**: Resources; **Xiao-Feng Yang**: Writing - Review & Editing; Project administration; Supervision.

Declaration of competing interest

The authors declare that they have no known competing financial interests or personal relationships that could have appeared to influence the work reported in this paper.

Acknowledgments

This research was supported by the National Natural Science Foundation of China (No. 22074120) and the Science and Innovation Capability Support Program of Shaanxi (No. 2020KJXX-030).

Appendix A. Supplementary data

Supplementary data to this article can be found online at https://doi.org/10.1016/j.dyepig.2021.109335.

References

[1] Kalyanaraman B, Cheng G, Hardy M, Ouari O, Bennett B, Zielonka J. Teaching the basics of reactive oxygen species and their relevance to cancer biology: mitochondrial reactive oxygen species detection, redox signaling, and targeted therapies. Redox Biol 2018;15:347–62.
[2] Rezende F, Brandes RP, Schröder K. Detection of hydrogen peroxide with fluorescent dyes. Antioxidants Redox Signal 2018;29:585–602.
[3] Lin MT, Beal MF. Mitochondrial dysfunction and oxidative stress in neurodegenerative diseases. Nature 2006;443:787–95.
[4] Brieger K, Schiavone S, Miller Jr FJ, Krause K-H. Reactive oxygen species: from health to disease. Swiss Med Wkly 2012;142:w13659.
[5] Zheng D-J, Yang Y-S, Zhu H-L. Recent progress in the development of small-molecule fluorescent probes for the detection of hydrogen peroxide. Trends Anal Chem 2019;118:625–51.
[6] Wen Y, Huo F, Yin C. Organelle targetable fluorescent probes for hydrogen peroxide. Chin Chem Lett 2019;30:1834–42.
[7] Bai X, Ng KK-H, Hu JJ, Ye S, Yang D. Small-molecule-based fluorescent sensors for selective detection of reactive oxygen species in biological systems. Annu Rev Biochem 2019;88:605–33.
[8] Chang MCY, Pralle A, Isacoff EY, Chang CJ. A selective, cell-permeable optical probe for hydrogen peroxide in living cells. J Am Chem Soc 2004;126:15392–3.
[9] Lippert AR, Van de Bittner GC, Chang CJ. Boronate oxidation as a bioorthogonal reaction approach for studying the chemistry of hydrogen peroxide in living systems. Acc Chem Res 2011;44:793–804.
[10] Abo M, Urano Y, Hanaoka K, Terai T, Komatsu T, Nagano T. Development of a highly sensitive fluorescence probe for hydrogen peroxide. J Am Chem Soc 2011;133:10629–37.
[11] Maeda H, Fukuyasu Y, Yoshida S, Fukuda M, Saeki K, Matsuno H, Yamauchi Y, Yoshida K, Hirata K, Miyamoto K. Fluorescent probes for hydrogen peroxide based on a non-oxidative mechanism. Angew Chem Int Ed 2004;43:2389–91.
[12] Xu K, Tang B, Huang H, Yang G, Chen Z, Li P, An L. Strong red fluorescent probes suitable for detecting hydrogen peroxide generated by mice peritoneal macrophages. Chem Commun 2005:5974–6.

[13] Xie X, Yang X, Wu T, Li Y, Li M, Tan Q, Wang X, Tang B. Rational design of an α-ketoamide-based near-infrared fluorescent probe specific for hydrogen peroxide in living systems. Anal Chem 2016;88:8019–25.
[14] Brewer TF, Garcia FJ, Onak CS, Carroll KS, Chang CJ. Chemical approaches to discovery and study of sources and targets of hydrogen peroxide redox signaling through NADPH oxidase proteins. Annu Rev Biochem 2015;84:765–90.
[15] Sikora A, Zielonka J, Lopez M, Joseph J, Kalyanaraman B. Direct oxidation of boronates by peroxynitrite: mechanism and implications in fluorescence imaging of peroxynitrite. Free Radical Biol Med 2009;47:1401–7.
[16] Chen X, Wang F, Hyun JY, Wei T, Qiang J, Ren X, Shin I, Yoon J. Recent progress in the development of fluorescent, luminescent and colorimetric probes for detection of reactive oxygen and nitrogen species. Chem Soc Rev 2016;45:2976–3016.
[17] Bezner BJ, Ryan LS, Lippert AR. Reaction-based luminescent probes for reactive sulfur, oxygen, and nitrogen species: analytical techniques and recent progress. Anal Chem 2020;92:309–26.
[18] Chen W, Li Z, Shi W, Ma H. A new resorufin-based spectroscopic probe for simple and sensitive detection of benzoyl peroxide via deboronation. Chem Commun 2012;48:2809–11.
[19] Cheng D, Xu W, Yuan L, Zhang X. Investigation of drug-induced hepatotoxicity and its remediation pathway with reaction-based fluorescent probes. Anal Chem 2017;89:7693–700.
[20] Li Y, Xie X, Yang X, Li M, Jiao X, Sun Y, Wang X, Tang B. Two-photon fluorescent probe for revealing drug-induced hepatotoxicity via mapping fluctuation of peroxynitrit. Chem Sci 2017;8:4006–11.
[21] Ye S, Hu J, Yang D. Tandem Payne/Dakin reaction: a new strategy for hydrogen peroxide detection and molecular imaging. Angew Chem Int Ed 2018;57:10173–7.
[22] Wu B, Yang J, Zhang J, Li Z, Li H, Yang X-F. A ratiometric fluorescent probe for the detection of endogenous hydroxyl radicals in living cells. Talanta 2019;196:317–24.
[23] Ye S, Hananya N, Green O, Chen H, Zhao A, Shen J, Shabat D, Yang D. A highly selective and sensitive chemiluminescent probe for real-time monitoring of hydrogen peroxide in cells and animals. Angew Chem Int Ed 2020;59:14326–30.
[24] Arias LA, Adkins S, Nagel CJ, Bach RD. Epoxidation of alkenes with trichloroacetonitrile/hydrogen peroxide in a neutral biphasic solvent system. J Org Chem 1983;48:888–90.
[25] Nad S, Kumbhakar M, Pal H. Photophysical properties of coumarin-152 and coumarin-481 dyes: unusual behavior in nonpolar and in higher polarity solvents. J Phys Chem A 2003;107:4808–16.
[26] Barik A, Kumbhaker M, Nath S, Pal H. Evidence for the TICT mediated nonradiative deexcitation process for the excited coumarin-1 dye in high polarity protic solvents. Chem Phys 2005;315:277–85.
[27] Raju BB, Varadarajan TS. Substituent and solvent effects on the twisted intramolecular charge transfer of three new 7-(diethylamino)coumarin-3-aldehyde derivatives. J Phys Chem 1994;98:8903–5.
[28] Cigáň M, Donovalová J, Szöcs V, Gapšar J, Jakusová K, Gáplovský A. 7-(Dimethylamino)coumarin-3-carbaldehyde and its phenylsemicarbazone: TICT excited state modulation, fluorescent H-aggregates, and preferential solvation. J Phys Chem A 2013;117:4870–83.
[29] Parker CA, Rees WT. Correction of fluorescence spectra and measurement of fluorescence quantum efficiency. Analyst 1960;85:587–600.
[30] Hocking MB, Ong JH. Kinetic studies of Dakin oxidation of o- and p-hydroxyacetophenones. Can J Chem 1977;55:102–10.
[31] Cheng X, Jia H, Feng J, Qin J, Li Z. Reactive" probe for hydrogen sulfite: "turn-on" fluorescent sensing and bioimaging application. J Mater Chem B 2013;1:4110–4.
[32] Kim T-K, Lee D-N, Kim H-J. Highly selective fluorescent sensor for homocysteine and cysteine. Tetrahedron Lett 2008;49:4879–81.
[33] Feuster EK, Glass TE. Detection of amines and unprotected amino acids in aqueous conditions by formation of highly fluorescent iminium ions. J Am Chem Soc 2003;125:16174–5.
[34] Xu C, Li H, Yin B. A colorimetric and ratiometric fluorescent probe for selective detection and cellular imaging of glutathione. Biosens Bioelectron 2015;72:275–81.
[35] Lee K-S, Kim H-J, Kim G-H, Shin I, Hong J-I. Fluorescent chemodosimeter for selective detection of cyanide in water. Org Lett 2008;10:49–51.
[36] Barooah N, Mohanty J, Pal H, Bhasikuttan AC. Non-covalent interactions of coumarin dyes with cucurbit uril macrocycle: modulation of ICT to TICT state conversion. Org Biomol Chem 2012;10:5055–62.
[37] Debnath T, Maity P, Lobo H, Singh B, Shankarling GS, Ghosh HN. Extensive reduction in back electron transfer in twisted intramolecular charge-transfer (TICT) coumarin-dye-sensitized TiO_2 nanoparticles/film: a femtosecond transient absorption study. Chem Eur J 2014;20:3510–9.
[38] Van Gompel JA, Schuster GB. Photophysical behavior of ester-substituted aminocoumarins: a new twist. J Phys Chem 1989;93:1292–5.
[39] Sun Q, Yang S-H, Wu L, Yang W-C, Yang G-F. A highly sensitive and selective fluorescent probe for thiophenol designed via a twist-blockage strategy. Anal Chem 2016;88:2266–72.
[40] Jones II G, Jackson WR, Choi CY, Bergmark WR. Solvent effects on emission yield and lifetime for coumarin laser dyes. Requirements for a rotatory decay mechanism. J Phys Chem 1985;89:294–300.
[41] Larsen EC, DiGennaro JA, Saito N, Mehta S, Loegering DJ, Mazurkiewicz JE, Lennartz MR. Differential requirement for classic and novel PKC isoforms in respiratory burst and phagocytosis in RAW 264.7 cells. J Immunol 2000;165:2809–17.
[42] Zhou Q, Liu C, Liu W, Zhang H, Zhang R, Liu J, Zhang J, Xu C, Liu L, Huang S, Chen L. Rotenone induction of hydrogen peroxide inhibits mTOR-mediated S6K1 and 4E-BP1/eIF4E pathways, leading to neuronal apoptosis. Toxicol Sci 2015;143:81–96.